

Electronic correlations in iron-pnictide superconductors and beyond; what can we learn from optics

L. Degiorgi¹

¹*Laboratorium für Festkörperphysik,
ETH - Zürich, CH-8093 Zürich, Switzerland*

(Dated: July 31, 2018)

Abstract

The Coulomb repulsion, impeding electrons' motion, has an important impact on the charge dynamics. It mainly causes a reduction of the effective metallic Drude weight (proportional to the so-called optical kinetic energy), encountered in the optical conductivity, with respect to the expectation within the nearly-free electron limit (defining the so-called band kinetic energy), as evinced from band-structure theory. In principle, the ratio between the optical and band kinetic energy allows defining the degree of electronic correlations. Through spectral weight arguments based on the excitation spectrum, we provide an experimental tool, free from any theoretical or band-structure based assumptions, in order to estimate the degree of electronic correlations in several systems. We first address the novel iron-pnictide superconductors, which serve to set the stage for our approach. We then revisit a large variety of materials, ranging from superconductors, to Kondo-like systems as well as materials close to the Mott-insulating state. As comparison we also tackle materials, where the electron-phonon coupling dominates. We establish a direct relationship between the strength of interaction and the resulting reduction of the optical kinetic energy of the itinerant charge carriers.

PACS numbers: 74.70.Xa,71.27.+a,71.10.Pm,78.20.-e

I. INTRODUCTION

Since the discovery of superconductivity in the iron-pnictide materials [1–4], the issue about the strength of their electronic correlations (i.e., the repulsive interactions among electrons) has been widely debated and it is still matter of intense investigations. This issue is of stringent importance for several families of (high temperature) superconductors, since superconductivity transition temperatures beyond 20 K cannot be yielded within conventional mechanism based on electron-phonon coupling [5]. In this respect, an ample discussion was also generated on whether the novel family of iron-pnictides does share common features and similarities with the high temperature superconducting cuprates (HTC), discovered more than 20 years ago [6]. In the cuprates electronic correlations are so strong that the parent compounds, out of which superconductivity originates, are Mott insulator. On the other hand, there is mounting evidence that the parent compounds of the iron-pnictide superconductors are bad metals, where electronic correlations are sufficiently strong to place them close to the boundary between itinerancy and interaction-induced electronic localizations [7]. Moreover in both families, superconductivity develops when magnetism, characterizing in part their phase diagram, is destroyed by dopings. This led to the conjecture that exchange of magnetic fluctuations may provide the glue, binding electrons into Cooper pairs [8].

The degree of electronic correlations has a direct impact on the charge dynamics, generally evinced from the optical conductivity [7, 9]. Thanks to the development of appropriate optical methods, this latter quantity can be achieved nowadays with great precision over an extremely broad spectral range, a prerequisite of paramount importance in order to track the implications of electronic correlations. Since electronic correlations significantly impede the mobility of the electrons, they consequently lead to a substantial reduction of the kinetic energy of the itinerant charge carriers with respect to the expectation for nearly-free or non-interacting particles. Precisely, one has to distinguish among two cases; namely, quenching the Drude weight by local (Hubbard-like) correlations or by interactions with a bosonic mode (i.e., phonons or spin fluctuations) [10]. The sum rule for the first case would reveal a spectral weight change from n/m_{LDA} (m_{LDA} being the crude mass for the local-density approximation (LDA)) to n/m_U (with m_U generally bigger than m_{LDA}). For

the second case, the sum rule would still lead to a total weight given by n/m_{LDA} , the latter being then redistributed between a Drude peak with weight proportional to n/m^* (m^* is the renormalized mass by the bosonic mode and is greater than m_{LDA}) and a so-called incoherent part encountering the remaining weight.

Qazilbash et al. recently made an interesting survey of the electronic correlations by looking to a wealth of materials, ranging from conventional metals to Mott insulators [11]. Along the same line of arguments previously introduced by Millis et al. (Ref. 12), they proposed a quantitative approach for the calculation of the ratio between the optical kinetic energy (K_{opt}) and the band kinetic energy (K_{band}). The former is obtained from the integral of the effective (Drude) metallic component of the optical conductivity (also referred as the coherent part of the single electron excitations in an interacting metallic system), while the latter quantity (also known as the kinetic energy of the underlying non-interacting system) is extracted from *ab initio* (tight-binding) band-structure calculations neglecting the electron-electron interactions [7]. Their analysis establishes a regime of moderate correlations for the iron-pnictide superconductors and leads to a nice correspondence between the degree of electronic correlations and the reduction of the empirical kinetic energy of the charge carriers compared with theory for a large variety of materials. Materials, for which the electron-phonon coupling predominately shapes the intrinsic physical properties, do not show, on the other hand, a significant reduction of the electrons' kinetic energy (Fig. 3 in Ref. 11).

Motivated by the work reported in Ref. 11, we undertook a systematic optical investigation of the Co-doped BaFe_2As_2 family, spanning the entire phase diagram [13]. We proposed to establish the ratio K_{opt}/K_{band} , exclusively from spectral weight arguments based on the experimental findings. The astonishing good correspondence of the degree of electronic correlations with the evolution of the superconducting phase in $\text{Ba}(\text{Co}_x\text{Fe}_{1-x})_2\text{As}_2$ (i.e., the superconducting dome defined by the T_c values in the phase diagram [14]), makes us confident that one can expand our procedure for other materials. The goal of this communication is to review our estimation of the electronic correlations across the phase diagram of the $\text{Ba}(\text{Co}_x\text{Fe}_{1-x})_2\text{As}_2$ compounds and place it in a broader context by revisiting from a similar perspective other variably correlated materials. We will compare the iron-pnictides

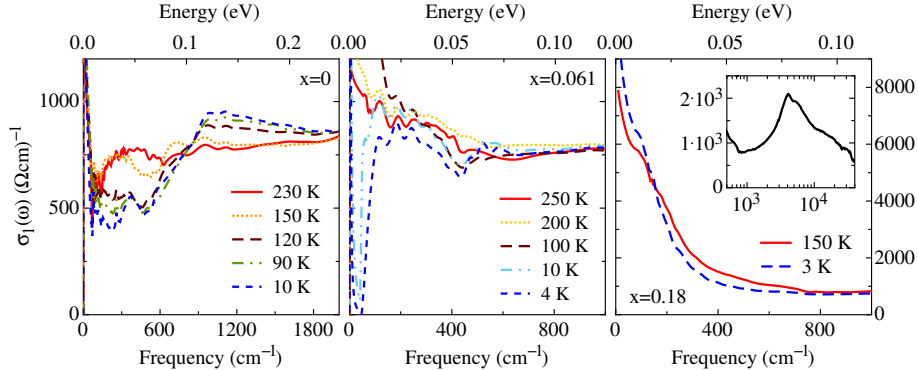


FIG. 1: (color online) Real part $\sigma_1(\omega)$ of the optical conductivity for $\text{Ba}(\text{Co}_x\text{Fe}_{1-x})_2\text{As}_2$ for $x = 0, 6.1\%$ and 18% in the far and mid-infrared spectral range at selected temperatures above and below the various phase transitions. The inset displays $\sigma_1(\omega)$ at 300 K for $x=18\%$, emphasizing its representative shape for all compounds at high frequencies up to the ultraviolet [13].

with other superconductors, like the HTC's and the boron-carbides and fullerenes, and with strongly correlated f - and d -electron systems (Kondo and heavy electron materials), as well as linear chain organic Bechgaard salts. Our review will be complemented with representative materials characterized by a CDW ground state, for which the electron-phonon coupling should dominate.

We show that an appropriate spectral-weight analysis can indeed reliably reveal the degree of electronic correlations and thus provide a valuable and exclusive experimental instruments, free from any *ad hoc* theoretical constrains, in order to discriminate among various systems with different levels of correlations. We principally analyze the real part ($\sigma_1(\omega)$) of the optical conductivity which is mainly obtained by first measuring the reflectivity ($R(\omega)$) over an extremely broad spectral range. This permits to perform reliable Kramers-Kronig transformation from which we calculate the phase of the complex reflectance and then all optical functions [15, 16].

II. EXPERIMENTAL RESULTS AND DISCUSSION

We start our survey by summarizing the most pertinent results on Co-doped BaFe_2As_2 , reported in Ref. 13 and which serve as an interesting case in point. Figure 1 shows $\sigma_1(\omega)$

in the far- and mid-infrared energy interval for selected Co-dopings (non-superconducting parent compound, optimal doping and non-superconducting overdoped compound) as a function of temperature. The parent compound ($x=0$) clearly displays the opening of the spin-density-wave (SDW)-pseudogap at T_{SDW} , while the optimally doped one ($x=6.1\%$) gives clear-cut evidence for the development of the superconducting gap below T_c . Finally, the compound ($x=18\%$) at the opposite end of the superconducting dome is in the metallic phase at all temperatures. Overall, there are three energy intervals characterizing $\sigma_1(\omega)$ for all Co-dopings: the effective metallic contribution at low frequencies, a rather flat mid-infrared (MIR) region covering the energy interval between 500 and 1500 cm^{-1} (from now on called MIR band) and the electronic interband transitions with onset at about 2000 cm^{-1} and peaked at 5000 cm^{-1} . The metallic part as well as the MIR band turn out to experience the strongest temperature dependence at T_c and/or T_{SDW} , while the high frequency excitations (inset Fig. 1) are temperature independent [13]. In order to account for the various contributions to the excitation spectrum, we applied the well-established phenomenological Drude-Lorentz approach [15, 16]. Besides high frequency Lorentz h.o.'s for the interband transitions with onset at $\omega \leq 2000 \text{ cm}^{-1}$ (inset Fig. 1), $\sigma_1(\omega)$ can be reproduced in great details by adding two Drude terms for the effective metallic contribution and a broad h.o. for the MIR energy interval (inset of Fig. 2) [13]. Consistent with Ref. 17, it turns out that one Drude term is rather narrow, while the second broad one acts as a background to the optical conductivity. These latter phenomenological components fully describe the temperature dependence of $\sigma_1(\omega)$ for all dopings (x). The two (narrow and broad) Drude terms imply the existence of two electronic subsystems. In passing, we remark that the approach is too phenomenological to allow speculations on whether the two Drude components have specific orbital character.

We proposed a scenario where the conduction band derives from d -states and splits into two parts: a purely itinerant one close to the Fermi level and represented by the two Drude components as well as by a bottom part with states below the mobility edge and thus rather localized [13]. This latter part gives rise to the MIR band in $\sigma_1(\omega)$, which turns out to be strongly temperature dependent upon magnetic ordering and affected by the opening of the SDW gap. In order to shed light on the relative distribution of spectral weight among the

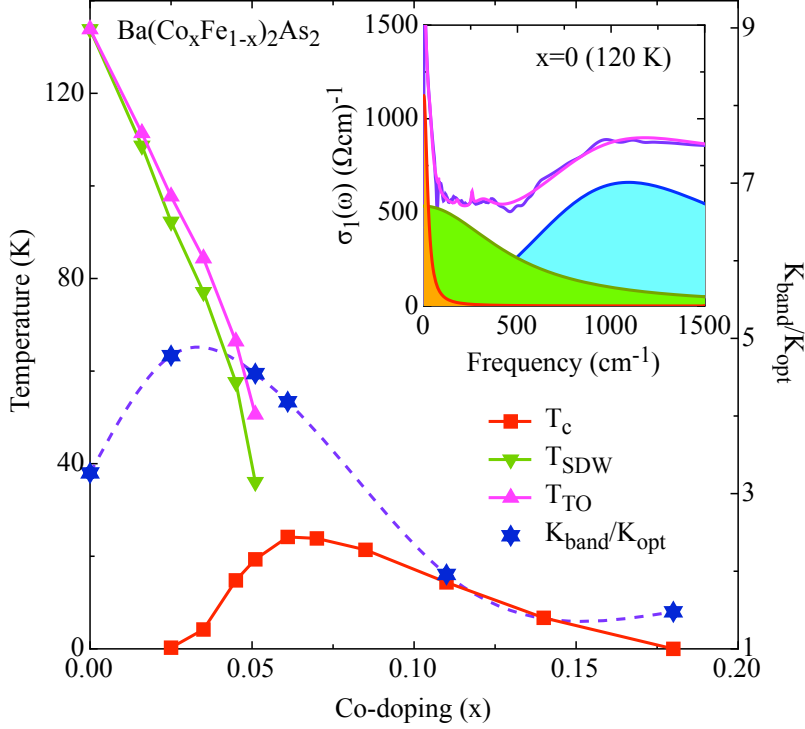


FIG. 2: (color online) Phase diagram of $\text{Ba}(\text{Co}_x\text{Fe}_{1-x})_2\text{As}_2$, reproduced from Ref. 14 (left y-axis), and the average of the ratio $K_{\text{band}}/K_{\text{opt}}$ (eq. (1)) calculated at high and low temperature (right y-axis). T_c , T_{SDW} and T_{TO} are the critical temperatures for the superconducting and SDW phase transition as well as for the tetragonal-orthorhombic structural transition, respectively [14]. All data-interpolation are spline lines as guide to the eyes. The inset displays the optical conductivity at 120 K for the parent compound ($x=0$) with the total Drude-Lorentz fit and its low frequency components; i.e., the narrow and broad Drude terms as well as the mid-infrared (MIR) h.o. (see text). The shaded areas emphasize the respective spectral weights ($\int \sigma_{1N}(\omega)d\omega$, $\int \sigma_{1B}(\omega)d\omega$ and $\int \sigma_1^{MIR}(\omega)d\omega$, eq. (1)) [13].

various (metallic and MIR) components of $\sigma_1(\omega)$, we have proposed to further exploit our phenomenological Drude-Lorentz description by calculating the spectral weight ratio:

$$K_{opt}/K_{band} = \frac{\int \sigma_{1N}(\omega)d\omega + \int \sigma_{1B}(\omega)d\omega}{\int \sigma_{1N}(\omega)d\omega + \int \sigma_{1B}(\omega)d\omega + \int \sigma_1^{MIR}(\omega)d\omega}, \quad (1)$$

where $\sigma_{1N}(\omega)$, $\sigma_{1B}(\omega)$ and $\sigma_1^{MIR}(\omega)$ are the fit components of the optical conductivity due to the narrow and broad Drude terms, and to the MIR band (inset of Fig. 2), respectively [13]. Equation (1) thus represents the ratio between the spectral weight encountered in $\sigma_1(\omega)$ in the Drude components (K_{opt}) and the total spectral weight collected in $\sigma_1(\omega)$ up to the onset of the electronic interband transitions (i.e., Drude components together with the MIR absorption feature, K_{band}). By assuming the conservation of the total charge carriers density, eq. (1) is in principle proportional to the ratio between the effective mass at low energy scales, which includes all renormalizations of local character or due to spin fluctuations, and at high energies, which only includes local effects of Hubbard type [18]. Therefore, the reduction of K_{opt} with respect to K_{band} (eq.(1)) would solely derive from the effective mass renormalization. Obviously in a multiband scenario as it applies in the iron-pnictides, it could well be that the rearrangement of the total number of charge carriers between hole and electron bands is such that the total charge carriers density is not conserved. In this case, the spectral weight reduction in the effective metallic contribution of $\sigma_1(\omega)$ might not be due to the effective mass (i.e., correlation effects) alone [19]. One should then carefully address the role of electron-electron interactions on both effective mass and charge carriers concentration. This is beyond the scope of the present discussion. As already emphasized above, our definition of K_{band} may be equivalent to the LDA expectation in the case that local Hubbard-like effects are negligible. Nevertheless, by assuming that the Hubbard renormalization factor would equally affect both K_{opt} and K_{band} , we are confident that eq. (1) is an alternative estimation, exclusively obtained from the experimental findings, of the ratio between the optical kinetic energy extracted by integrating $\sigma_1(\omega)$ up to the onset of the electronic interband transitions [11] and the band kinetic energy extracted from the band structure within the tight-binding approach. We are also aware of the fact that the MIR band may be also contaminated by coherent contributions originating from transitions between bands close to the Fermi level (in the case of the iron-pnictides of hole-hole type) or

by the low energy tail contribution of high energy interband transitions. We assume those effects to be small. We have calculated K_{opt}/K_{band} after eq. (1) at high and low temperature, yet still corresponding to the normal or SDW state [20]. Our K_{opt}/K_{band} for $x=0$ is consistent with the value reported in Fig. 3 of Ref. 11 for the same compound, therefore reinforcing the validity of our spectral weight arguments. The inverse of K_{opt}/K_{band} , which then defines the degree of electronic correlations, is plotted in Fig. 2 as average of the K_{band}/K_{opt} values at low and high temperature [20] within the phase diagram of the Co-doped 122 iron-pnictides [14]. K_{band}/K_{opt} thus tracks the evolution of its superconducting dome. Interestingly enough, electronic correlations seem to be stronger for the parent-compound and for Co-dopings $x \leq 0.061$ than for those in the overdoped range. There is indeed evidence for a crossover from a regime of moderate correlations for $x \leq 0.061$ to a nearly-free and non-interacting electron gas system for $x \geq 0.11$ [13].

With the goal to further generalize our approach towards the estimation of K_{opt}/K_{band} based on the spectral weight analysis of $\sigma_1(\omega)$ (eq. (1)), we recollect first of all the electrodynamic response of two other families of superconductors: the alkali-doped fullerenes (AC_{60} , $A=K, Rb$ and Cs) and the boroncarbides LNi_2B_2C ($L=Lu, Tm, Er, Ho, Dy$ and Y). Their electrodynamic response [21, 22] in the normal state shares general features with $\sigma_1(\omega)$ of the HTC's (see below) [9] and iron-pnictides, as well. The normal state $\sigma_1(\omega)$ of YNi_2B_2C and K_3C_{60} is reproduced in Fig. 3. There is evidence for a two component picture: a Drude response up to ω_{opt} , getting narrow with decreasing temperature, and a mid-infrared band, extending up to ω_{band} [23] and being reminiscent of a pseudogap-like excitation. Only about 10% of the total weight (i.e., $K_{opt}/K_{band} \sim 0.1$, [24]), encountered in $\sigma_1(\omega)$ up to the onset of the electronic interband transitions, can be ascribed to the itinerant charge carriers. This would imply that both the superconducting fullerenes and boroncarbides are strongly correlated materials at the verge of a Mott insulating state. K_{opt}/K_{band} for both systems are summarized in our figure of merit (Fig. 4), allowing a first comparison with values previously achieved for the iron-pnictides (Fig. 2).

It is now compelling to compare the degree of electronic correlations between these latter families of superconductors and the high-temperature copper-oxides. For the purpose of our discussion, we consider the partial, yet representative series of the underdoped

Bi₂Sr₂CaCu₂O_{8+δ} (Bi2212 (UD), $T_c=67$ K), the optimally doped YBa₂Cu₃O_{*x*} (Y123 (OP), $T_c=93.5$ K) and the overdoped Tl₂Sr₂CuO_{6+δ} (Tl2201 (OD), $T_c=23$ K) compounds [9, 25]. The integral of $\sigma_1(\omega)$ up to the onset of the electronic interband transitions (at about $\omega_{band} \sim 1$ eV) leads to the total spectral weight proportional to K_{band} after eq. (1). The effective Drude weight, which then defines our K_{opt} , is obtained by integrating $\sigma_1(\omega)$ up to a cut-off frequency $\omega_{opt} \sim 1000$ cm⁻¹, thus at the onset of the pseudogap excitation [23–25]. The ratio K_{opt}/K_{band} is summarized in Fig. 4 for the three chosen compounds and results to be fully in trend with our arguments, proposed above for the iron-pnictides and other superconductors. Our results are even in fair agreement with a semi-theoretical approach on the electron and hole doped cuprates, reported in Refs. 9 and 12. It is worth noting, that $\sigma_1(\omega)$ in the non-superconducting La_{2-*x*}Sr_{*x*}CuO₄ ($x=0.26$) [26] is characterized by a simple Drude response without any signature of the pseudogap excitation, thus implying $K_{opt}/K_{band} \sim 1$ (eq. (1)). This is fully consistent with a nearly-free electron limit, as expected for conventional metals like Au or Al [16, 27].

The linear chain organic Bechgaard salts [28] were also intensively investigated, because of their rich phase diagram. At low temperatures, they provide an interesting arena in which to study the pressure (chemical and applied) induced crossover between a spin-Peierls, a SDW and a superconducting state. At high temperatures one can study the dimensionality-driven evolution between a Mott insulating and an incipient Fermi liquid state upon compressing the lattice. We have shown that the optical conductivity in the metallic state of (TMTSF)₂X (where X= SF₆, AsF₆ or ClO₄) is highly anisotropic and display dramatic deviations from a simple Drude response [29, 30]. Figure 3 displays, as an example, $\sigma_1(\omega)$ for X=PF₆ at 300 and 20 K. One can appreciate the emergence of two prominent features with decreasing temperature: a narrow mode at zero frequency, with a small amount of spectral weight, and a mode centered around 200 cm⁻¹, with nearly all the spectral weight expected for the relevant number of carriers and single particle band mass (Fig. 3). We argued that these features are characteristic of a quasi one-dimensional half- or quarter-filled band with Coulomb correlations, and ascribed the finite-energy mode to the correlation (pesudo)gap. We proposed a scenario consistent with a doped Mott-semiconducting behavior of the organic Bechgaard salts [29, 30]. The interchain coupling, represented by the transverse charge

transfer integral (t_{\perp}) between the chains, induces indeed a self-doping of the Mott insulating state of the strict one-dimensional limit (i.e., $t_{\perp}=0$), thus populating the upper Hubbard band and leading to the tiny Drude weight encountered in the zero energy resonance of $\sigma_1(\omega)$ (Fig. 3). K_{opt}/K_{band} corresponds here to the ratio between the spectral weight of the zero energy mode for $\omega < \omega_{opt} \sim 20 \text{ cm}^{-1}$ (i.e., about 1% of the total weight) and the total weight of both the zero- and finite-energy modes, up to $\omega_{band} \sim 4000 \text{ cm}^{-1}$ [23]. This results in $K_{opt}/K_{band} \sim 0.008$ (Fig. 4) [24], which is again consistent with the Mott-limit.

Another interesting class of correlated systems is the family of heavy-electron (HE) and more generally Kondo-like materials. Electron-electron interaction leads to two characteristic excitations: a renormalized Drude response and a mid-infrared peak [31, 32]. The latter originates from a dynamical, correlation-induced gap, as evinced from a many body theoretical approach based on the periodic Anderson model [33]. At low temperatures, it can be viewed as optical gap between two renormalized quasi-particle bands. Paramount examples of HEs are CeAl_3 , CePd_3 and UPt_3 , just to name a few. Figure 3 displays $\sigma_1(\omega)$ above and below the Kondo temperature T_K for CeAl_3 [34]. The spectrum above T_K is compatible with a simple Drude response up to $\omega_{band} \sim 4000 \text{ cm}^{-1}$ and can be used to estimate K_{band} in eq. (1), while $\sigma_1(\omega)$ below T_K is characterized by the narrow Drude contribution up to $\omega_{opt} \sim 60 \text{ cm}^{-1}$, due to the effective mass renormalization [23]. The spectral weight of such a renormalized Drude response defines K_{opt} . K_{opt}/K_{band} in prototype HEs oscillates between 0.003 and 0.02 [24]; i.e., only about 0.3 to 2 % of the expected total spectral weight in the nearly-free electron or simple band-metal limit is effectively encountered in the (narrow) Drude response of $\sigma_1(\omega)$ [31–34]. These values of K_{opt}/K_{band} also place the HE systems within the strongly correlated regime, comparable to the situation of the Mott-like insulating state (Fig. 4). It is worth noting that our experimental estimation of K_{opt}/K_{band} is particularly suitable in this context. In fact, it is not plagued by the annoying role of the localized f -electrons, which would make K_{band} from band-structure calculations less trustable and poorly reliable.

Among the highly correlated electron systems, various rare-earth compounds known as hybridization-gap semiconductors or Kondo insulators [31, 35] have also attracted considerable interest recently. The cubic compound FeSi is a prominent example, particularly

suitable for investigating aspects of the electronic properties of a d -transition metal system that might be related with features of correlation effects in f -electron materials. At low frequencies, an Anderson-Mott localization behavior was established from the optical conductivity, while at high frequencies the excitation spectrum resembles that of a conventional semiconductor [36]. Figure 3 displays $\sigma_1(\omega)$ of FeSi at 300 K, which is characterized by a metallic contribution below $\omega_{opt} \sim 500 \text{ cm}^{-1}$ and by a broad bump peaked at about 700 cm^{-1} and extending up to $\omega_{band} \sim 1500 \text{ cm}^{-1}$ [23, 24]. The latter feature is an incipient hybridization induced pseudogap, which evolves in the semiconducting gap excitation at low temperatures (e.g., at 10 K, Fig. 3) [36]. The ratio of the spectral weight belonging to the metallic state with respect to the total one (eq. (1)), including the semiconducting mid-infrared gap, leads to K_{opt}/K_{band} of about 0.4 (Fig. 4), thus placing FeSi in the regime of moderate electronic correlations.

Materials exhibiting colossal magnetoresistive effect are of high current interest in solid state physics, primarily because of potential technological applications. The well-known manganites and Ca-doped EuB_6 , for which the onset of ferromagnetism is accompanied by a dramatic reduction of the electrical resistivity, have intensively been studied. With magneto-optical investigations on the $\text{Eu}_{1-x}\text{Ca}_x\text{B}_6$ series [37, 38] we revealed a phase diagram in support of a scenario based on the double-exchange model [39]. That model foresees the close proximity of the Fermi level and a magnetization dependent mobility edge so that a ferromagnetic metal-(Anderson) insulator transition (at $T = 0$) occurs upon increasing the Ca-content above a critical Ca concentration (x_{MI}) of about 0.5. The Ca-doping induces a drift of the mobility edge such that above x_{MI} it goes past the Fermi energy and the spin polarization due to the ferromagnetic transition no longer releases any of the localized states. The Drude weight is thus insensitive to the spin polarization above x_{MI} [39]. The fingerprint of such a metal-insulator crossover (at $T > 0$) was tracked by the spectral weight changes in the Drude component as a function of both magnetic field and temperature [39]. The optical conductivity $\sigma_1(\omega)$ above the ferromagnetic transition of selected $\text{Eu}_{1-x}\text{Ca}_x\text{B}_6$, shown in Fig. 3, gives evidence for a metallic component up to $\omega_{opt} \sim 300 \text{ cm}^{-1}$, with a broad high frequency tail, extending up to $\omega_{band} \sim 2000 \text{ cm}^{-1}$ and due to localized charge carriers. We can calculate K_{opt}/K_{band} (eq. (1)) for selected Ca-dopings by considering the ratio between

the effective metallic (Drude) spectral weight (i.e., up to the cut-off energy ω_{opt}) and the overall one encountered in $\sigma_1(\omega)$ below ω_{band} [23], thus including the excitations due to the charge carriers located below the mobility edge [24]. Figure 4 shows K_{opt}/K_{band} for $x=0$, 0.3 (i.e., $x \leq x_{MI}$) and $x=0.8$ (i.e., $x \geq x_{MI}$). Upon increasing the Ca-content, the optical response across the ferromagnetic metal-insulator transition mimics the evolution which would be expected for a crossover between the moderate and strong electronic correlations' regimes.

We conclude our survey by addressing the broken symmetry ground state due to the formation of a charge-density-wave (CDW) condensate, which derives from the Peierls transition [40]. The paradigm of CDW forming materials are the quasi-one-dimensional (1D) compounds but electronically driven CDW states were also found in novel two-dimensional (2D) layered compounds [41]. The physics of low-dimensional CDW systems recently experienced a revival of interest. Particularly 2D CDW materials were thoroughly re-investigated, an effort motivated in part by the fact that high-temperature superconductivity in the cuprates may emerge from a peculiar charge ordering in 2D through the tuning of relevant parameters [42]. In Fig. 3 we display $\sigma_1(\omega)$ for a prototype layered CDW system, ErTe_3 , both in the normal and CDW state [43]. Above the CDW transition temperature (T_{CDW}) besides the metallic contribution up to ω_{opt} there is a broad mid-infrared high energy tail up to ω_{band} [23]. In quasi-1D CDW materials, like the well-known $\text{K}_{0.3}\text{MoO}_3$, the broad mid-infrared feature clearly appears as a pseudogap-like excitation [44]. This latter feature, developing above T_{CDW} , is ascribed to a precursor CDW gap because of fluctuation effects and evolves into the CDW single-particle excitation below T_{CDW} (Fig. 3). Therefore, K_{band} after eq. (1) results from the total spectral weight, given by the sum of the effective metallic contribution (then defining K_{opt}) and the weight encountered in the MIR feature due to the Fermi surface gapping as consequence of the CDW precursor effects. For typical 1D materials, like $\text{K}_{0.3}\text{MoO}_3$, the resulting K_{opt}/K_{band} is astonishingly small, of the order of 0.1, while for the 2D rare-earth tritellurides, as ErTe_3 or HoTe_3 , is of about 0.8-1 (Fig. 4). This would imply that the reduction of the electrons' kinetic energy is negligible in 2D materials, as usually expected when electron-phonon coupling is at work. That K_{opt}/K_{band} is, on the other hand, substantially reduced in truly chain-like 1D systems possibly originates from an

extremely strong electron-phonon coupling, leading to the formation of polarons [45]. The interesting case of 1D CDW materials allows us to broaden the notion of reduced kinetic energy not only as a consequence of electron-electron but also of electron-phonon interaction, thus generalizing the impact of interactions on the charge dynamics as well as ultimately the concept of correlation.

III. CONCLUSION

The present survey over a large wealth of materials provides a rather clear-cut evidence for a direct relationship between the strength of interaction (electron-electron as well as electron-phonon) and the experimentally evinced reduction of the (Drude) metallic spectral weight in the excitation spectrum. The total spectral weight encountered in the optical conductivity up to the onset of the electronic interband transitions turns out to be usually redistributed into a well-distinct Drude resonance and a so-called incoherent part, identified throughout the paper with the generic MIR band concept. We consequently figure out that the stronger is the Coulomb repulsion or the electron-phonon coupling, the stronger is the deviation of the charge-dynamics from a simple band-metal response, pushing the materials into the strongly correlated regime which is comparable with a Mott-insulating or a polaron's dominated state, respectively.

Since the origin of interactions may be very diverse, the physical meaning of the MIR feature, due to the incoherent part of $\sigma_1(\omega)$, is also very different from system to system. Similarly, the reduced Drude weight, as effective integrated quantity, may originate from changes of the charge density as well as of the mass enhancement of the itinerant carriers, depending from the physics involved in the investigated material. We made the assumption that the effective (reduced) Drude weight should be compared to the total one encountered in $\sigma_1(\omega)$ below the interband transitions. However, it remains to be seen, how the total weight up to ω_{band} deviates from the LDA expectation in the nearly-free electron limit. Nevertheless, we believe that our definition of the degree of electronic correlations from spectral weight argument in terms of the K_{opt}/K_{band} ratio would be little influenced by those deviations, thus representing a truly experimental and reliable method towards its estimation.

Acknowledgments

The author wishes to thank A. Lucarelli, M. Dressel, L. Benfatto, D. Basov, M. Qazilbash and A. Chubukov for fruitful discussions. This work has been supported by the Swiss National Foundation for the Scientific Research within the NCCR MaNEP pool.

-
- [1] Y. Kamihara et al., *J. Am. Chem. Soc.* **130**, 3296 (2008).
 - [2] M. Rotter et al., *Phys. Rev. Lett.* **101**, 107006 (2008).
 - [3] X.H. Chen et al., *Nature* **453**, 761 (2008).
 - [4] A.S. Sefat et al., *Phys. Rev. Lett.* **101**, 117004 (2008).
 - [5] M. Tinkham, *Introduction to superconductivity*, 2nd Ed., McGraw-Hill, New York (1996).
 - [6] J.G. Bednorz et al., *Z. Phys. B* **64**, 189 (1986).
 - [7] Q. Si, *Nature Physics* **5**, 629 (2009).
 - [8] I.I. Mazin, *Nature* **464**, 183 (2010).
 - [9] D.N. Basov and T. Timusk, *Rev. Mod. Phys.* **77**, 721 (2005), and references therein.
 - [10] L. Benfatto, private communication.
 - [11] M.M. Qazilbash et al., *Nature Physics* **5**, 647 (2009).
 - [12] A.J. Millis et al., *Phys. Rev. B* **72**, 224517 (2005).
 - [13] A. Lucarelli et al., *cond-mat/1004.3022*.
 - [14] J.-H. Chu et al., *Phys. Rev. B* **79**, 014506 (2009) and references therein.
 - [15] F. Wooten, *Optical Properties of Solids*, Academic Press, New York (1972).
 - [16] M. Dressel and G. Grüner, *Electrodynamics of Solids*, Cambridge University Press (2002).
 - [17] D. Wu et al., *Phys. Rev. B* **81**, 100512(R) (2010).
 - [18] L. Benfatto et al., *Phys. Rev. B* **80**, 214522 (2009).
 - [19] L. Ortenzi et al., *Phys. Rev. Lett.* **103**, 046404 (2009).
 - [20] That superconductivity in the iron-pnictides emerges in close proximity of an antiferromagnetic (AF) ground state implies the important role of AF fluctuations for the pairing mechanism of all itinerant charge carriers. Both Drude terms are affected by the superconducting

transition [17] and it is consequently legitimate to consider the total spectral weight of both of them (i.e., involving all ungapped charge carriers) for the definition of the optical kinetic energy. For low Co-dopings (particularly for $x \leq 0.025$), the SDW instability and the resulting Fermi surface gapping at low temperatures within the SDW state obviously leads to a reshuffling of spectral weight, thus affecting both quantities K_{opt} and K_{band} in eq. (1). Therefore, K_{opt}/K_{band} after eq. (1) for the underdoped compounds ($x \leq 0.025$) is smaller at $T < T_{SDW}$ than above. Nevertheless, it turns out that K_{band}/K_{opt} both at high and low temperature behaves similarly as a function of Co-doping, so that both estimations converge with increasing doping-content and are basically identical for $x \geq 0.11$. Thus, the proposed average value in Fig. 2 suitably gives an overall trend for the degree of electronic correlations.

- [21] L. Degiorgi, *Adv. Phys.* **47**, 207 (1998), and references therein.
- [22] F. Bommeli et al., *Phys. Rev. Lett.* **78**, 547 (1997).
- [23] By Drude response, we intend the truly metallic component in $\sigma_1(\omega)$, generally reproduced by a simple Drude term [15, 16]. Such a Drude term is usually well distinct up to a cut-off frequency ω_{opt} . On the other hand, ω_{band} denotes the onset of the electronic interband transitions and it is generally defined as the zero-crossing energy of the imaginary part of the complex optical conductivity [11].
- [24] $K_{opt} \sim \int_0^{\omega_{opt}} \sigma_1(\omega) d\omega$ and $K_{band} \sim \int_0^{\omega_{band}} \sigma_1(\omega) d\omega$ (Fig. 3). Alternatively, one can exploit the phenomenological Drude-Lorentz fit [15, 16], so that $K_{opt} \sim \omega_p^2$ and $K_{band} \sim \omega_p^2 + \sum_j S_j^2$ (ω_p being the plasma frequency of the effective Drude term shaping $\sigma_1(\omega)$ up to ω_{opt} and S_j^2 the mode strength of the j -Lorentz h.o.'s contributing to $\sigma_1(\omega)$ up to ω_{band}). Details to the fits and related parameters can be evinced for each material from the quoted references.
- [25] A.V. Puchkov et al., *J. Phys.: Condens. Matter* **8**, 10049 (1996), and references therein.
- [26] A. Lucarelli et al., *Phys. Rev. Lett.* **90**, 037002 (2003).
- [27] The $\sigma_1(\omega)$ spectrum of conventional metals, like Au and Al, can be reproduced by a simple Drude response, the integral of which leads to values of the plasma frequency $\omega_p \sim \sqrt{n/m_e}$, totally in agreement with the theoretical expectation given by the charge carrier concentration (n) from chemical counting and the free electron mass (m_e) [16].
- [28] D. Jerome and H.J. Schulz, *Adv. Phys* **31**, 299 (1982).

- [29] A. Schwartz et al., *Phys. Rev. B* **58**, 1261 (1998).
- [30] V. Vescoli et al., *Science* **281**, 1155 (1998).
- [31] L. Degiorgi, *Rev. Mod. Phys.* **71**, 687 (1999) and references therein.
- [32] L. Degiorgi et al., *Z. Phys. B* **102**, 367 (1997).
- [33] L. Degiorgi et al., *Eur. Phys. J. B* **19**, 167 (2001).
- [34] A.M. Awasthi et al., *Phys. Rev. B* **48**, 10692 (1993).
- [35] G. Aeppli and Z. Fisk, *Comments Condens. Matter Phys.* **16**, 155 (1992).
- [36] L. Degiorgi et al., *Europhys. Lett* **28**, 341 (1994).
- [37] L. Degiorgi et al., *Phys. Rev. Lett.* **79**, 5134 (1997).
- [38] S. Broderick et al., *Phys. Rev. B* **65**, 121102(R) (2002).
- [39] G. Caimi et al., *Phys. Rev. Lett.* **96**, 016403 (2006) and references therein.
- [40] G. Grüner, *Density Waves in Solids*, Addison Wesley, Reading, MA (1994).
- [41] J. Rouxel, in *Crystal Chemistry and Properties of Materials with quasi-one-dimensional Structures*, Editor J. Rouxel, D. Reidel Publishing Company, Dordrecht (1986), pp. 1-26.
- [42] see section V in: S.A. Kivelson et al., *Rev. Mod. Phys.* **75**, 1201 (2003).
- [43] F. Pfuner et al., *Phys. Rev. B* **81**, 195110 (2010).
- [44] A. Schwartz et al., *Phys. Rev. B* **52**, 5643 (1995).
- [45] L. Perfetti et al., *Phys. Rev. Lett.* **87**, 216404 (2001).

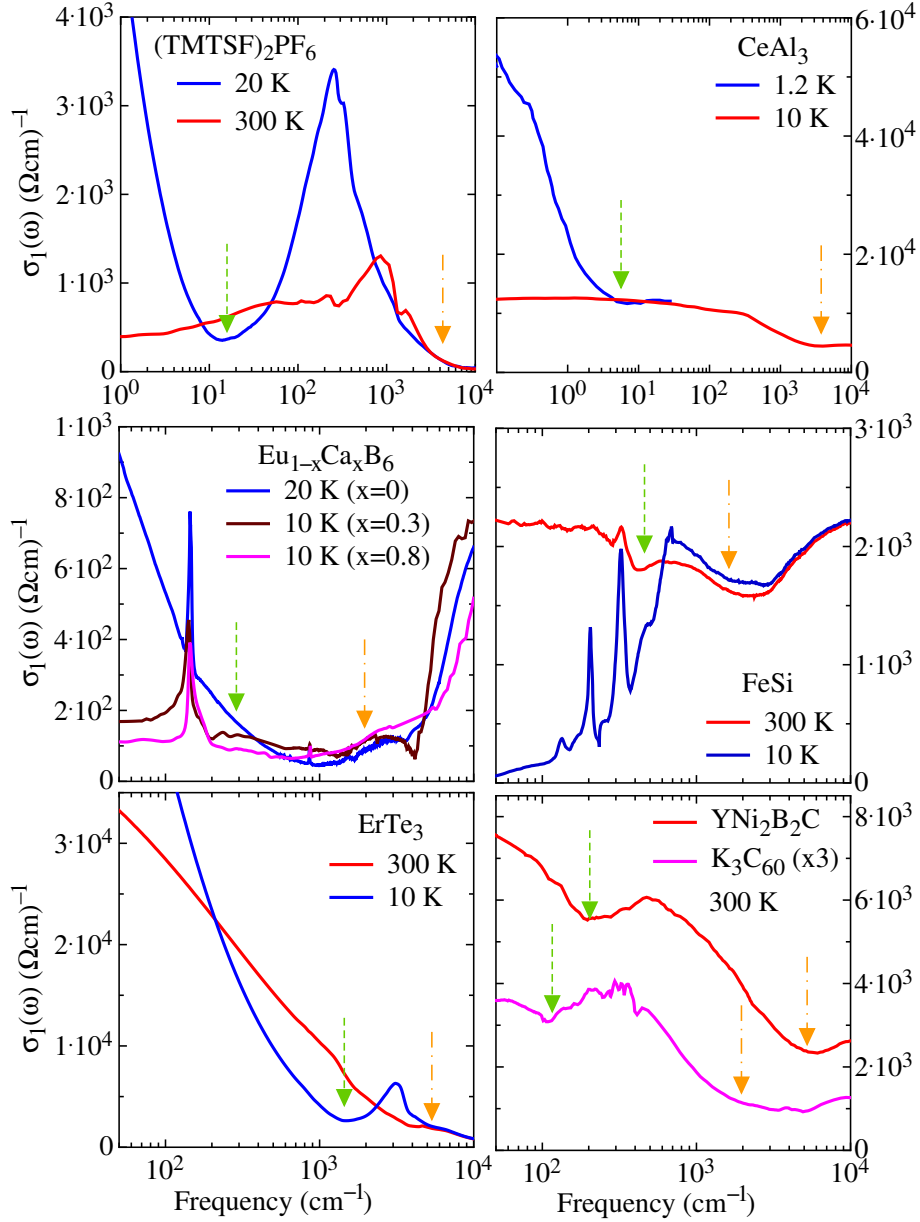


FIG. 3: (color online) Real part $\sigma_1(\omega)$ of the optical conductivity at selected temperatures for the linear chain Bechgaard salt $(\text{TMTSF})_2\text{PF}_6$ [29, 30], the heavy-electron CeAl_3 [34], the ferromagnetic metal $\text{Eu}_{1-x}\text{Ca}_x\text{B}_6$ for $x=0, 0.3$ and 0.8 [37, 39], the Kondo insulator FeSi [36], the CDW rare-earth tritellurides ErTe_3 [43] and the superconducting boroncarbide $\text{YNi}_2\text{B}_2\text{C}$ [22] and K_3C_{60} [21] (for clarity $\sigma_1(\omega)$ has been here multiplied by a factor of three). Please note the different frequency scales for $(\text{TMTSF})_2\text{PF}_6$ and CeAl_3 , which extend into the microwave spectral range. The dashed and dashed-dotted arrows mark the cut-off frequencies ω_{opt} and ω_{band} (see text) of the integrated optical conductivity leading to K_{opt} and K_{band} , respectively [7, 11, 23, 24].

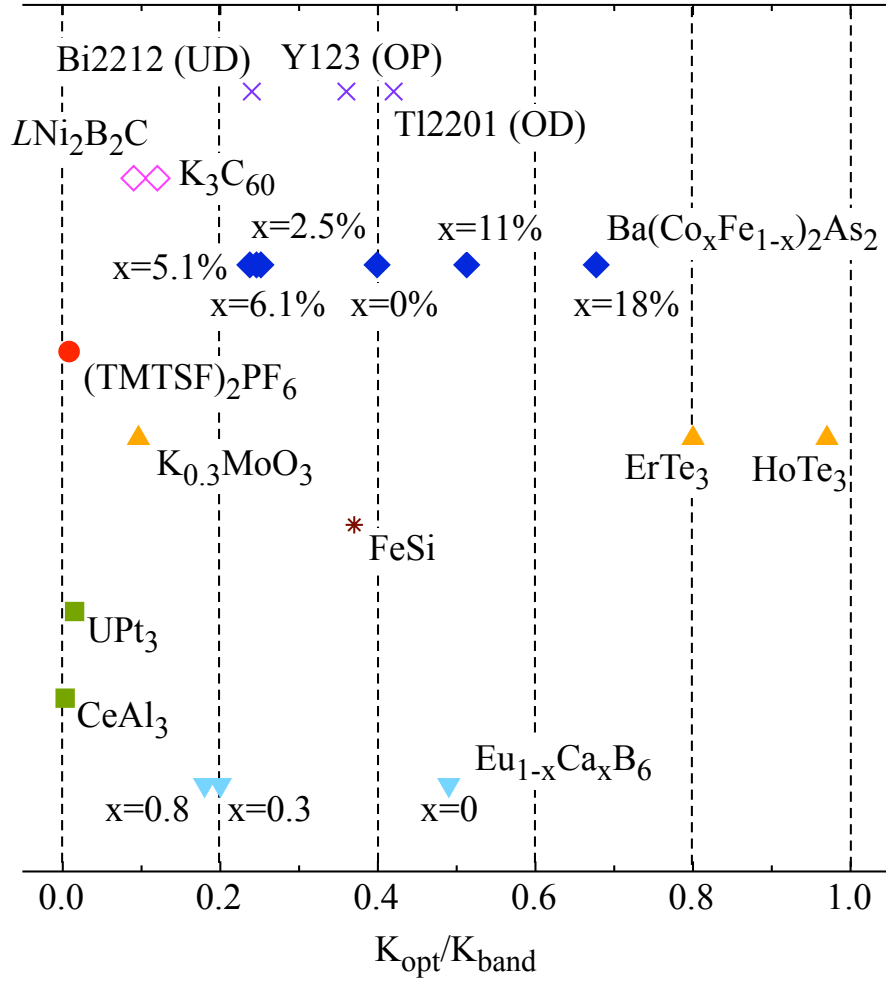


FIG. 4: (color online) The ratio K_{opt}/K_{band} (eq. (1)) calculated for selected materials, spanning a broad range of the degree of electronic correlations (see text).